

# Reversible and Efficient Light-Induced Molecular Switching on an Insulator Surface

Simon Jaekel,<sup>1</sup> Antje Richter,<sup>2</sup> Robert Lindner,<sup>2</sup> Ralf Bechstein,<sup>2</sup> Christophe Nacci,<sup>1</sup>

Stefan Hecht,<sup>3</sup> Angelika Kühnle,<sup>2</sup> and Leonhard Grill<sup>1\*</sup>

*1) Department of Physical Chemistry, University of Graz, Heinrichstrasse 28, Graz, Austria*

*2) Department of Physical Chemistry, University of Mainz, Duesbergweg 10-14, Mainz, Germany*

*3) Department of Chemistry, Humboldt-Universität zu Berlin, Brook-Taylor-Str. 2, Berlin, Germany*

\* Corresponding author: leonhard.grill@uni-graz.at

## Contents

Manipulation of molecular islands with the AFM tip	p. S2
Contrast dependence on AFM imaging parameters	p. S3
Total coverage	p. S3
UV/vis light source	p. S5
Illumination ports	p. S5
Deposition of M-TBA onto the cold Au(111) surface	p. S6
Molecular geometry from single-crystal x-ray diffraction	p. S7
Isomerization cross sections	p. S8
References	p. S10

### Manipulation of molecular islands with the AFM tip

The *trans* layer of M-TBA molecules can be manipulated by approaching the AFM tip (*i.e.* increasing the  $\Delta f$  set point) towards the sample. Figure S1 shows an example if the surface scanned in this way (at  $\Delta f = 19.0\text{Hz}$  as compared to  $\Delta f = 17.0\text{Hz}$  during normal imaging).

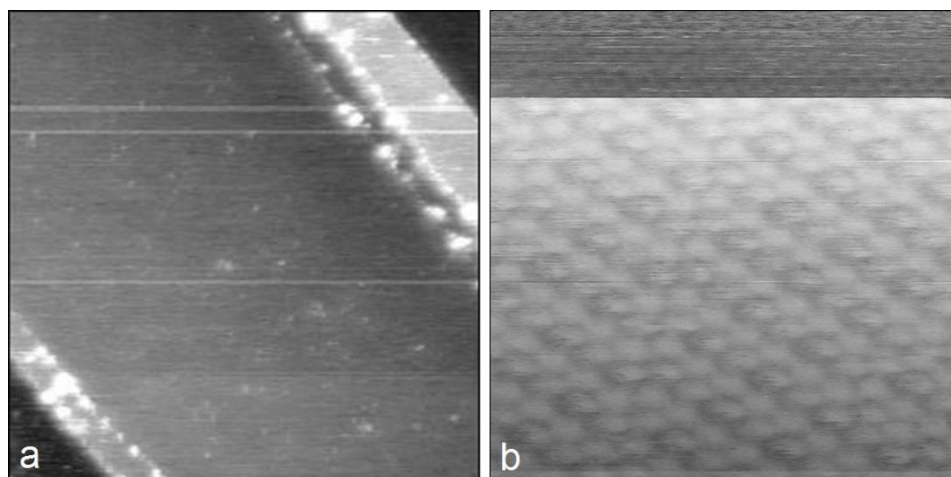


Fig. S1: (a) AFM image (at constant  $\Delta f$ ) of M-TBA molecules on the calcite ( $\text{CaCO}_3$ ) ( $10\bar{1}4$ ) surface before manipulation. Image size:  $256 \times 256 \text{ nm}^2$ . (b) Zoom-in AFM image (image size:  $16 \times 16 \text{ nm}^2$ ) with scanning in horizontal lines from bottom to top. In the last segment of the image (darker area at the top) the  $\Delta f$  set point is increased, thus approaching the tip which pushes away the molecules and resolves the calcite surface.

As a result of these changed imaging parameters an improved resolution is obtained as the molecules are pushed aside and the bare calcite surface becomes visible (Fig. S2). Note that the range of  $\Delta f$  values for which stable imaging or manipulation occurs depends strongly on the precise tip conditions. For sharp tips manipulation can occur as early as 9.0 Hz and more, while blunter tips can be scanned with about 50 Hz to 60 Hz before the layer is disturbed.

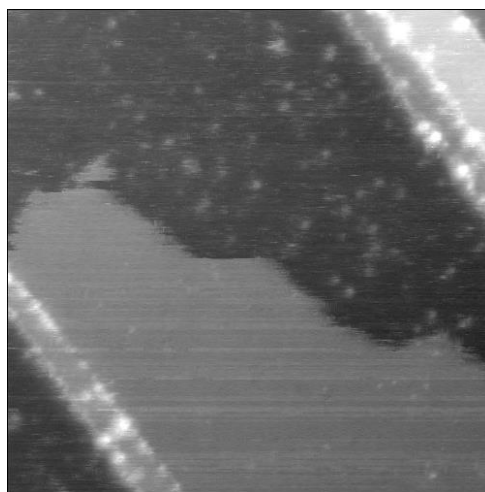


Fig. S2: Constant- $\Delta f$  AFM image (image size:  $256 \times 256 \text{ nm}^2$ ) after manipulation.

As shown in Fig. S2 scanning the same area after the manipulation event shows only the revealed calcite and the remains of the old MTBA layer, but no structures with intermediate height.

### Contrast dependence on AFM imaging parameters

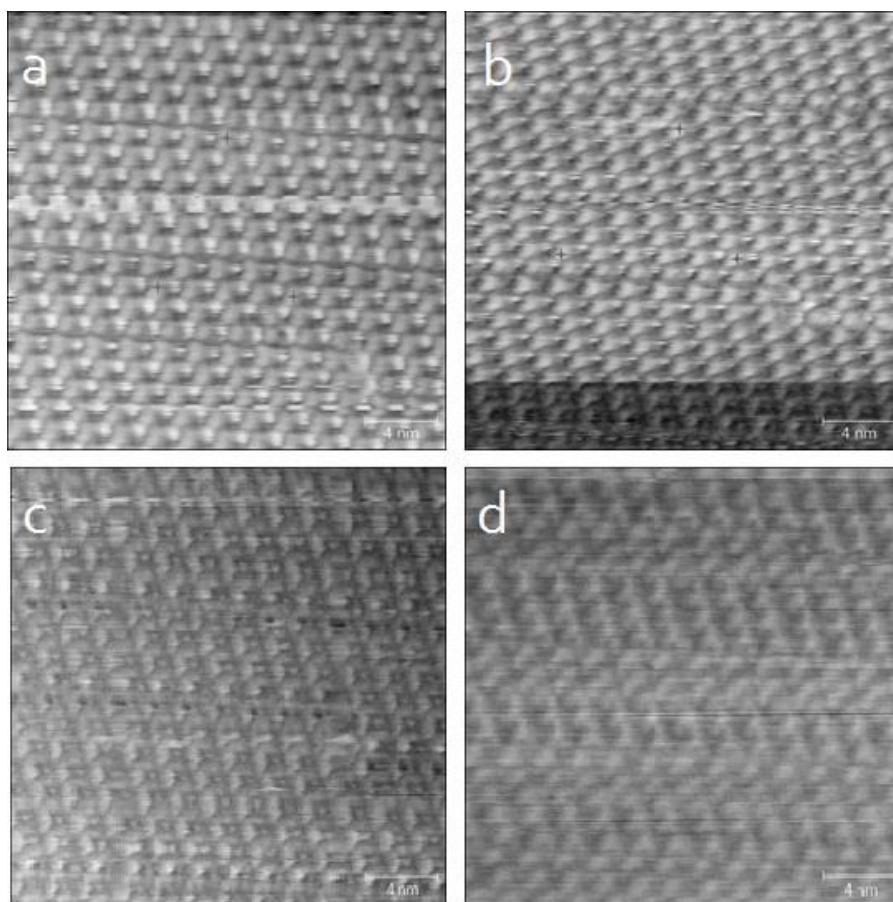


Fig. S3: Series of constant- $\Delta f$  AFM images (all  $24 \times 24 \text{ nm}^2$  in size) of one and the same surface area with varying set points and contrasts.  $\Delta f$  set point values: (a) 6.1 Hz, (b) 7.0 Hz (and 7.6 Hz during scanning at the bottom), (c) 8.1 Hz and (d) 9.9 Hz.

As shown in Fig. S3, the contrast for the *trans* layer of MTBA depends strongly on the  $\Delta f$  set point. Further, any combination of  $\Delta f$  value and resolution applies only to one AFM tip and will not be replicated with a different tip.

### Total coverage

The total molecular coverage decreases during illumination. We fitted this process over time (Fig. S4 and S5) with a simple exponential function

$$c(t) = c_0 \cdot \exp(-t/\tau)$$

(which describes desorption with a single time constant) where  $t$  is the time,  $c$  is the coverage per surface area,  $c_0$  is the starting coverage (at  $t=0$ ) and  $\tau$  is the decay time.

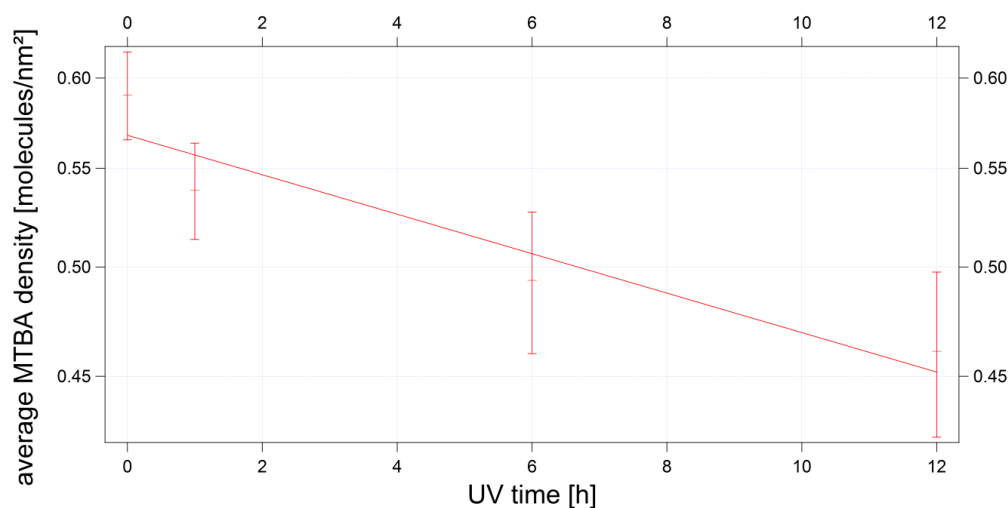


Fig. S4: Logarithmic plot of the total M-TBA coverage during illumination with UV/vis light. The line shows a fit of the data with a simple exponential function (as described in the text).

Our data (Fig. S4 and S5) shows that this simple equation is in agreement with the experimental data. However, the error bars are rather large, which means that a more complex desorption mechanism can neither be ruled out nor confirmed within the margin of error and the time covered by the dataset ( $t < \tau$ ). Note that this is valid for both light sources, UV/vis light (Fig. S4) and 450 nm laser light (Fig. S5). The decay constants of the fitted functions are  $(53 \pm 14)$ h for the UV/vis light and  $(340 \pm 30)$ s for the laser light.

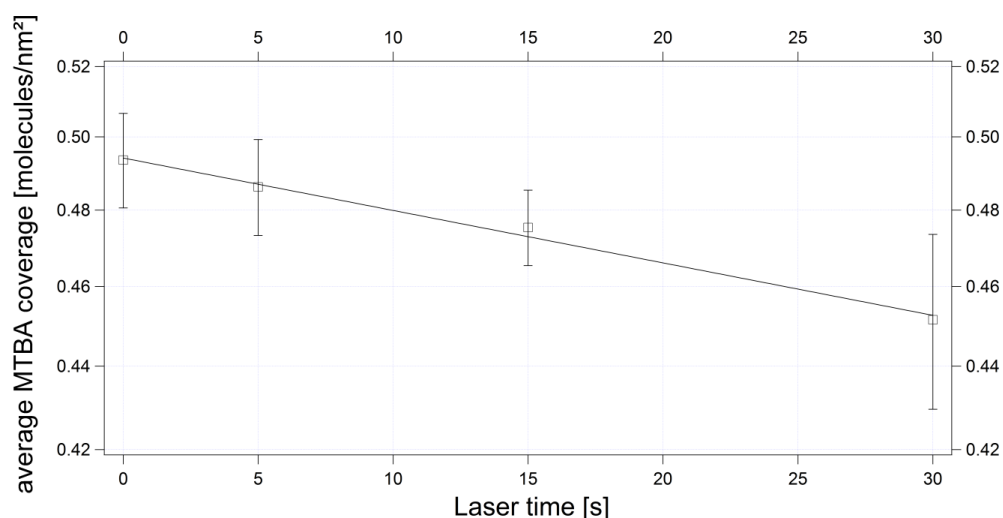


Fig. S5: Logarithmic plot of the total MTBA coverage during illumination with 450 nm laser light. The line shows a fit of the data with a simple exponential function (as described in the text).

### UV/vis light source

The spectrum of the UV/vis light source used for the illumination experiments is plotted in Fig.S6. The power density is  $3.09 \text{ mW/cm}^2$ , the total photon density is  $7.9 \times 10^{15} \text{ s}^{-1}\text{cm}^{-2}$  with the major density at higher energies (photon density up to 550 nm:  $4.0 \times 10^{15} \text{ s}^{-1}\text{cm}^{-2}$ ).

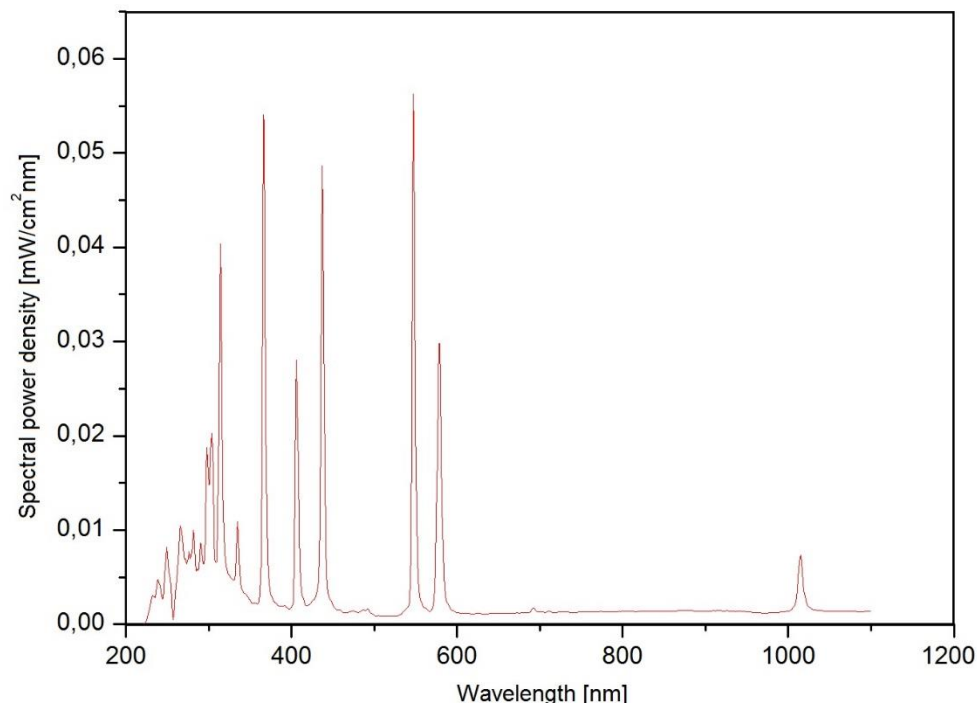


Fig. S6: Spectral power density (at a distance of 37 cm from the lamp, i.e. the sample position) of the Hg lamp used for UV/vis illumination.

### Illumination ports

The optical transmission properties of the windows used for UV/vis and laser illumination are shown in Fig. S7 and S8.

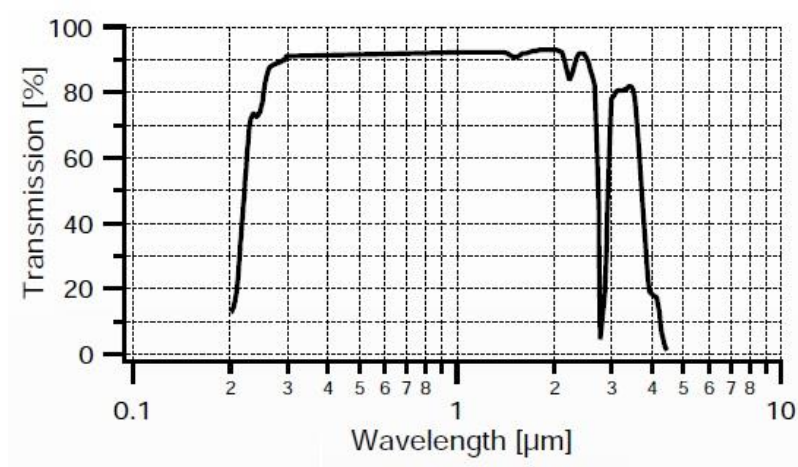


Fig. S7: Optical transmission of the fused silica window (Silux®) through which the sample was illuminated by the UV/vis lamp.

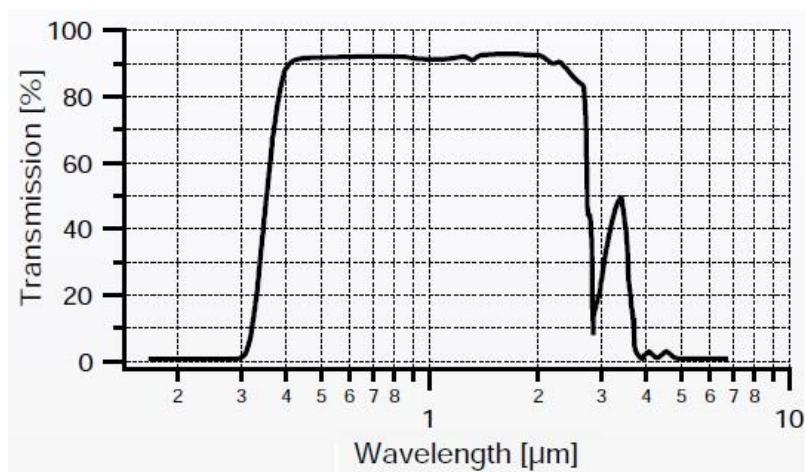


Fig. S8: Optical transmission of the borosilicate window (Borofloat® 33) through which the sample was illuminated by the 450 nm laser.

### Deposition of M-TBA onto the cold Au(111) surface

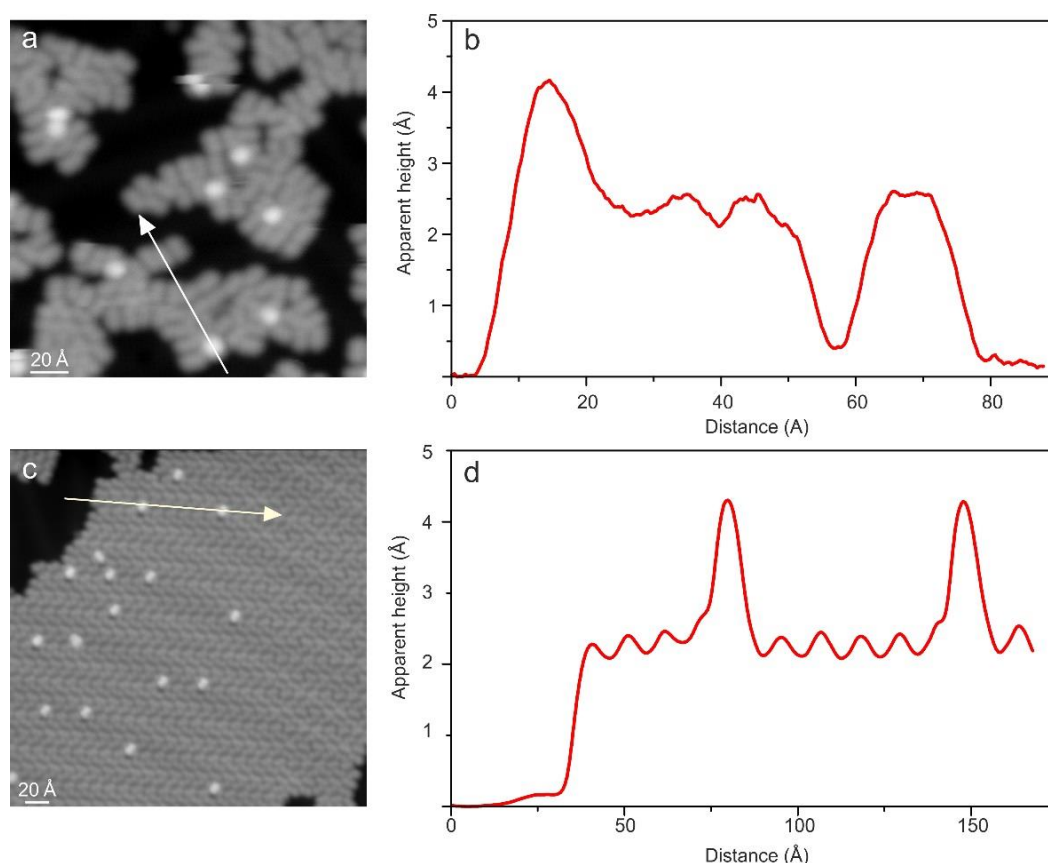


Fig. S9: (a) STM image (1 V, 0.2 pA) of M-TBA molecules deposited onto the Au(111) surface kept at 10 K during deposition with (b) the corresponding height profile over molecules of different brightnesses (along the arrow in the STM image). (c) STM image (1 V, 0.2 nA) of M-TBA molecules deposited onto the Au(111) surface kept at 220 K during deposition and switched to the cis state by voltage pulses [1] with (d) the corresponding height profile over trans (dark) and cis (bright) molecules (along the arrow in the STM image).



If M-TBA molecules are deposited onto a Au(111) surface at low temperature (10 K), *cis* isomers can be identified directly after the preparation (Fig.S9a-b). These *cis* isomers are identified by their characteristic appearance in STM images: From deposition of M-TBA onto Au(111) at 220 K and subsequent switching to the *cis* state by voltage pulses [1], the apparent height of *cis* isomers in STM images is determined (Fig.S9c-d) as  $4.22 \pm 0.15$  Å (for a bias voltage of 1V at the sample). This is in very good agreement with the preparation at low temperatures (Fig.S9a-b) where characteristic apparent heights of  $4.19 \pm 0.15$  Å (at the same bias voltage of 1V on the sample) are found. At the same time, the darker molecules (*trans* isomers) appear in both cases at a height of about 2.6 Å (Fig.S9b and d) [1]. Hence, dark and bright lobes after preparation at low temperatures indeed correspond to *trans* and *cis* isomers, respectively.

The observation of *cis* isomers directly after deposition onto Au(111) is in contrast to experiments with the same molecules on Au(111) kept at higher temperatures (220 K) during preparation, where exclusively *trans* isomers are present [1]. A rough estimation shows that about 10% of the molecules are in the *cis* state at cold preparation, which is in agreement with the 18% that are found on the calcite surface after preparation at room temperature. We therefore conclude that *cis* isomers are present in the gas phase and these are preserved upon landing on the cold Au(111) surface, but thermally all relax to the *trans* state if the sample is at room temperature [1]. On the other hand, the calcite surface traps these *cis* isomers kinetically and therefore preserves the gas phase distribution of *trans* and *cis* isomers (Fig.2f in the main text).

### Molecular geometry from single-crystal x-ray diffraction

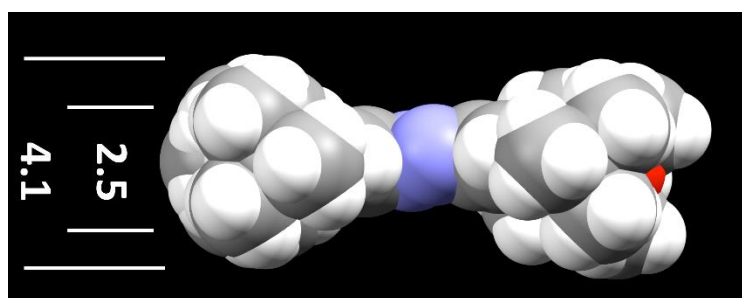


Fig. S10: Rendering of the molecular geometry (side-view) of *cis*-MTBA in the solid as obtained from X-ray diffraction data of the molecular crystal. Marked distances are extremal H-H and C-C distances (in Å) within the tert-butyl moieties. Carbon in grey; Nitrogen in blue; Oxygen in red; Hydrogen in white. As commonly observed for these systems, rotational disorders of three tert-butyl moieties were observed as well as a disorder of the methoxy substituent. The structure was refined accordingly using geometric restraints prohibiting the use of error bars since disorders were idealized. One tert-butyl moiety shows no disorder, the distances were determined to be 2.489(6) (C23–C24) and 2.483(6) (C24–C25) Å.

The molecular geometry can be used to gain reference values for the expected thickness of a single molecular layer. We have determined this geometry from X-ray diffraction data on a single-crystal of *trans*-MTBA (Fig. S10, [2]). Note that in a flat adsorption geometry the thickest point of a layer can be expected to correspond to the effective height of the *tert*-butyl groups. Comparison with apparent heights as obtained from AFM measurements should be considered with some care because of the different interactions between the neighboring molecules in the crystal vs. molecules on the surface.

The lateral packing dimensions can also be estimated from the crystal structure by evaluating the molecular dimensions including vdW-radii as shown in Fig. S11. The 9 Å distance along the shorter edge takes into account that the molecules will interlock within the packing, because of their non-uniform width in this direction.

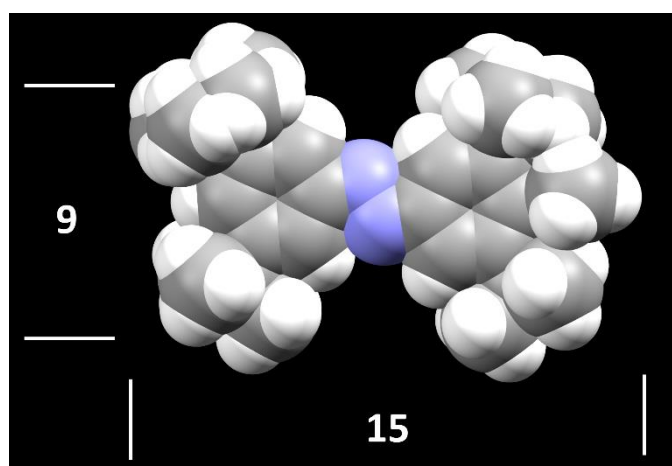


Fig. S11: Rendering of the molecular geometry (top-view) in the solid phase of *cis*-MTBA obtained from X-ray diffraction data of the molecular crystal. Marked distances give rough estimates of the space requirements (in Å) in dense 2D packing. Carbon in grey; Nitrogen in blue; Hydrogen in white (Oxygen not visible in top-view).

### Isomerization cross sections

Isomerization cross sections  $\Phi_C$  (isomerization from *cis* to *trans* isomer) and  $\Phi_T$  (isomerization from *trans* to *cis* isomer) are determined from evaluating the concentration of the *cis* isomer  $C(n)$  in dependence of the photon exposure.

Assuming a first-order equilibrium reaction  $T(n) \leftrightarrow C(n)$  is given by

$$C(n) = T(0) \frac{\Phi_T}{\Phi_C + \Phi_T} (1 - e^{-(\Phi_C + \Phi_T)n}) + C(0) \frac{1}{\Phi_C + \Phi_T} (\Phi_T + \Phi_C e^{-(\Phi_C + \Phi_T)n})$$

$$C(n) = e^{-(\Phi_C + \Phi_T)n} \left( C(0) \frac{\Phi_C}{\Phi_C + \Phi_T} - T(0) \frac{\Phi_T}{\Phi_C + \Phi_T} \right) + (T(0) + C(0)) \frac{\Phi_T}{\Phi_C + \Phi_T}$$



$$C(n) = A \cdot e^{-(\Phi_C + \Phi_T)n} + C_{pss}$$

where  $C(n)$  is the concentration of *cis* isomers,  $T(n)$  is the concentration of *trans* isomers,  $C(0), T(0)$  are the initial concentrations,  $C_{pss}$  is the concentration in the photostationary state,  $n$  is the photon exposure, and  $A = \left( C(0) \frac{\Phi_C}{\Phi_C + \Phi_T} - T(0) \frac{\Phi_T}{\Phi_C + \Phi_T} \right)$ .

Treating  $A$  as an initial state dependent constant, the values of  $\Phi_C + \Phi_T$  and  $C_{pss}$  can be extracted from the data:  $\Phi_C + \Phi_T = (6.39 \pm 1.43) \times 10^{-20} \text{ cm}^2$  and  $C_{pss} = 0.552 \pm 0.019$  for the UV/vis illumination;  $\Phi_C + \Phi_T = (7.25 \pm 0.74) \times 10^{-18} \text{ cm}^2$  and  $C_{pss} = 0.198 \pm 0.006$  for the 455 nm laser illumination.

Individual cross sections are extracted from  $\Phi_C + \Phi_T$  through the equation  $C_{pss} = \frac{\Phi_T}{\Phi_T + \Phi_C}$ .

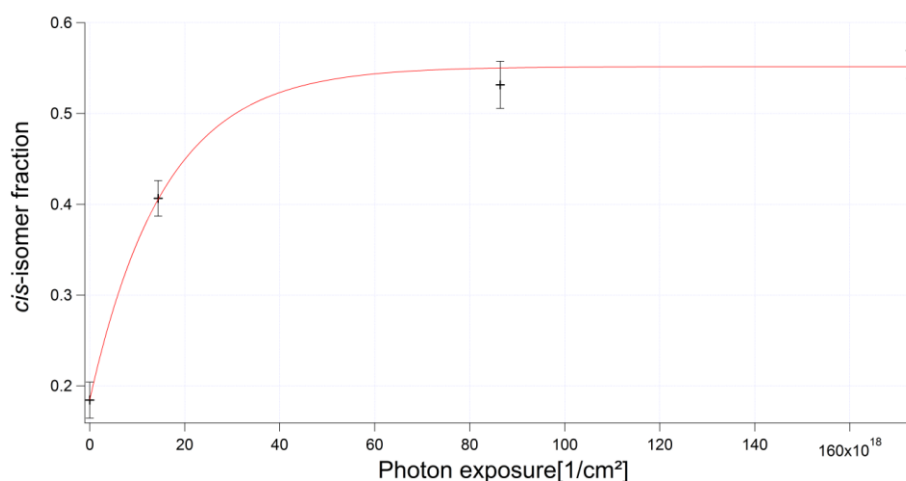


Fig. S12: Plot of the fraction of MTBA molecules in the *cis* conformation dependent on exposure to UV/vis light. Exponential fit used to determine the isomerization cross section in red.

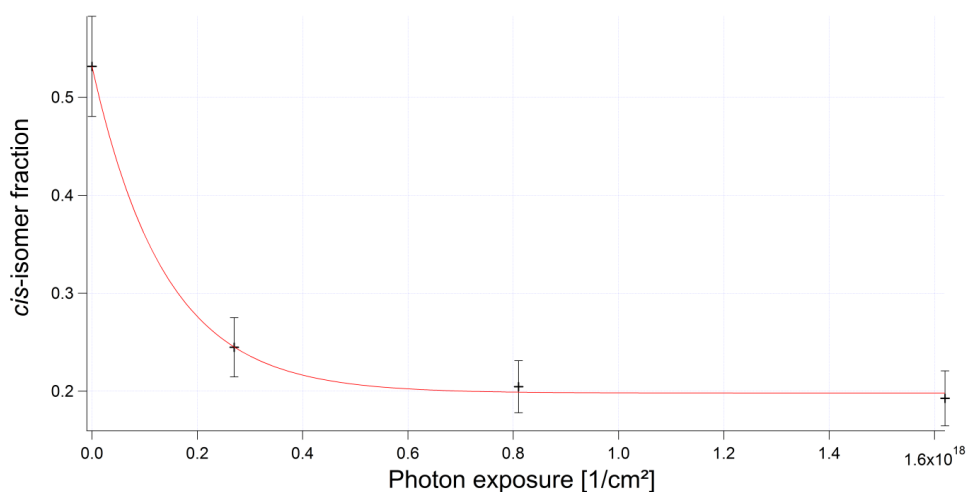


Fig. S13: Plot of the fraction of MTBA molecules in the *cis* conformation dependent on exposure to 450nm laser light. Exponential fit used to determine the isomerization cross section in red.

## **References**

- [1] C. Dri, M. V. Peters, J. Schwarz, S. Hecht, and L. Grill, Spatial Periodicity in Molecular Switching, *Nat. Nanotechnol.* **3**, 649 (2008).
- [2] C. Dri, M. V. Peters, J. Schwarz, S. Hecht, and L. Grill, Spatial Periodicity in Molecular Switching, Supporting Information of *Nat. Nanotechnol.* **3**, 649 (2008).